Effect of Cement Kiln Bypass Dust on Properties and Hydration of Akali-Activated Slag Mixtures

Vlastimil Bílek[a], Lukáš Kalina[b], Radoslav Novotný[c], Jiří Másilko[d], František Šoukal[e]

Faculty of Chemistry, Materials Research Centre, Brno University of Technology, Brno, Czech Republic

[a]bilek@fch.vut.cz
[b]kalina@fch.vut.cz
[c]xcnovotny2@fch.vut.cz
[d]masilko@fch.vut.cz
[e]soukal@fch.vut.cz

ABSTRACT

During recent decades, alkali-activated slag (AAS) systems have attracted great scientific interest around the world. Despite many efforts its severe shrinkage and cracking is still a delicate issue. The aim of this work was to partially replace slag by cement kiln bypass dust (CBPD) which, on the basis of its mineralogical composition, would act as an expansive agent (EA) and thus compensate AAS shrinkage. It was observed that volume changes of AAS/CBPD mixtures strongly depended on CBPD dose since low slag replacement levels did not significantly reduce autogenous shrinkage while around 50% of CBPD or more led to severe expansion. Based on X-ray diffraction, this expansion is related to hydrocalumite-type phase formation. The presence of CBPD also totally modified calorimetric response of AAS pastes.

1. Introduction

Alkali-activated slag (AAS)-based systems as an alternative for traditional Portland cement-based systems attracted significant scientific attention during the several recent decades. AAS is claimed to have excellent mechanical properties and durability, but its wider use is limited particularly by missing standards and severe drying and autogenous shrinkage together with cracking tendency. Plenty of approaches how to mitigate AAS shrinkage have been used, e.g. curing at elevated temperatures, internal curing, blending of slag with other mineral additives or the use of shrinkage-reducing admixtures.

Another possibility is an application of expansive agents (EAs), i.e. the substances whose hydration results in the formation of products causing an expansion of the material. Most often used EAs are calcium sulphoaluminate or dead burn CaO. The expansive mechanism of the former is based on ettringite formation while the latter produces portlandite. Because separate weighing of EAs during the concrete production is impractical and problems with precise dosing can arise, they are usually mixed with Portland cement to obtain so called shrinkage compensating cements used for the production of shrinkage compensating concretes. Shrinkage compensation lies in sufficient initial expansion of these concretes to compensate for subsequent drying shrinkage. The expansion takes place during the first days of wet or water curing and causes compressive stresses in the material (chemical prestress) which are not as dangerous as tensile stresses developed during the subsequent stages of drying shrinkage. Thanks to the initial chemical prestress, tensile stresses do not exceed tensile strength of the material which prevents cracking (Aïtcin & Flatt 2015).

Some studies dealing with the use of expansive agents in AAS can be found in literature. Yuan et al. (2014) used the mixture of quick lime, periclase and anhydrite at the doses of 0–8% with respect to the slag weight. Increasing dose of the EA resulted in significant drying shrinkage decrease with 75% shrinkage reduction for 8% of EA. Authors claimed that such shrinkage reduction can be related to the presence of portlandite, which was found in all samples on XRD, while ettringite was not detected, although it was formed in the mixture of EA with activating solution and water (without slag). Nevertheless, high doses of EA worsened workability and had strong accelerating effect on setting times which were shorter even than 10 minutes in some cases.

Another authors (Jin et al. 2014) applied two forms of MgO with different reactivity as an EA at the doses of 0–7.5% with respect to the slag weight. The more reactive form of MgO was effective in shrinkage reduction particularly during the first days; shrinkage was reduced by approximately 25% for 7.5% of MgO. The less reactive form of MgO had only slight effect on shrinkage with its maximum reduction of 13%. Regardless the form and dose of MgO, specimens had high cracking tendency during the first days while later self-healing effect was observed in some specimens, particularly for the those containing less reactive form of MgO. Beneficial effect on shrinkage was related to the formation of hydrotalcite-like phases, while brucite was not detected in this case. Also in Shen et al. (2011), beneficial effect of MgO on shrinkage and cracking of blended alkali-activated slag and fly ash mixtures was observed but in this case related mainly to the brucite formation.

It can be summarized that only few papers dealing with the use of EAs in AAS with sometimes contradictory results have been published. For this reason, cement kiln bypass dust (CBPD) containing some phases with expansive potential was used as an admixture partially replacing slag in AAS pastes and mortars. The effect of CBPD not only on volume changes of AAS but also on its setting time and hydration was investigated.

2. Expertimental part

2.1 Materials and mixture composition

Ground granulated blast furnace slag (BFS) with Blaine fineness of 400 m^2/kg was used as a starting aluminosilicate precursor. It was predominantly composed of amorphous phase with traces of crystalline minerals calcite, merwinite and akermanite/gehlenite as determined using X-ray diffraction method (XRD) with Rietveld analysis and calcium fluoride as an internal standard. BFS was partially or

in some extreme cases even fully replaced by CBPD, which was rich in free CaO (~35%), KCl (~35%) and larnite (~22%), contained amorphous phase and also some minor crystalline phases like arcanite, akermanite-gehlenite and quartz. BFS replacement level by CBPD was used to distinguish the mixtures, e.g. CBPD-30 was mixture containing 30% of CBPD and 70% of BFS. Both BFS and CBPD were considered being the binder for the purposes of mixture designing. Also reference mixtures (Ref.) without CBPD were tested.

Waterglass with silicate modulus of 2.0 was used as an alkaline activator. Its dose was adjusted to 4% of Na_2O with respect to the binder weight. Water to binder ratio including water from waterglass was 0.35 for pastes and 0.46 for mortars. Sand to binder ratio was 2 : 1 using siliceous sand with maximum grain size of 2 mm as prescribed for cement testing according to EN 196-1. When possible, mixing procedure was also inspired by EN 196-1.

2.2 Testing procedures

2.2.1 Setting time

Initial and final setting times were determined using Vicat apparatus commonly used for Portland cement characterization (EN 196-3). The testing was performed at laboratory conditions (~25 °C and ~50% of relative humidity).

2.2.2 Compressive strength

Compressive strength was determined at the ages of 24 hours, 7 days and 28 days on the halves of the moist cured specimens with dimensions of 20 mm × 20 mm × 100 mm after the flexural strength test. Six values for compressive strength were obtained for each mixture at each age and averaged.

2.2.3 Autogenous volume changes

Volume changes at autogenous conditions were determined using hydrostatic weighing method. Latex condoms were filled with the paste (~75 g), tied with fishing line and hanged on balances. First of all, weight on air m_{air} was recorded and then the specimen was immersed in oil and its weight recorded every minute for several days. Assuming that temperature of oil and thus its density is constant during the measurement, volume change in percent ΔV was calculated using (1), where $m_{oil,ini}$ is initial weight of the specimen in oil and $m_{oil,t}$ is weight of the specimen in oil at any time.

$$\Delta V = \frac{m_{oil,ini} - m_{oil,t}}{m_{air} - m_{oil,ini}} \cdot 100 \quad (1)$$

2.2.4 Isothermal calorimetry

Effect of CBPD on hydration of AAS was determined using isothermal calorimetry. To reliably record the heat flow also during the initial stages of hydration, “Admix” ampoules, i.e. 20ml glass vials equipped with a syringe and a special teflon stirrer, were used. This enabled separate preconditioning of the binder (in a vial) and activating solution (in a syringe) inside the calorimeter to the temperature of the measurement (25 °C). After that, activating solution was, still in-situ, added to the binder and mixed for three minutes. Heat of hydration was recorded from the first contact of the activating solution with the binder.

2.2.5 X-ray diffraction

To support the results from the methods described above, mixture with BFS/CBPD = 50/50 was selected to determine its phase composition evolution in time using PANanalytical Empyrean device. Before the measurement started specimens were crushed and mixed with excess of isopropyl alcohol for one hour to stop their hydration. Then they were dried at the temperature of 40 °C for two hours and refined using vibrating mill for 15 seconds. The XRD measurement was performed in Bragg-Brentano configuration at the range of 5–90° 2θ, X-ray tube with copper anode with voltage of 30 kV and electric current of 40 mA was used. The obtained data were evaluated using PDF2 database. Reference codes of the detected phases are given in appendix.

3. Results and discussion

The effect of CBPD on setting time and compressive strength is given in Figure 1. It can be seen that increasing BFS replacement by CBPD resulted in a gradual shortening of both initial and final setting time. Also volume changes in autogenous conditions were strongly dependent on the BFS replacement level as can be seen in Figure 2. In some cases (0 and 50% of CBPD) the test was repeated to check its reproducibility. For the lowest CBPD doses, i.e. 10 and 20%, no or slight reduction in autogenous shrinkage was observed, while the use of 30% CBPD led to noticeable expansion with its maximum at approx. 18 hours followed by shrinking. Further increase in CBPD dose up to 50 and 100% resulted in strong expansion: around 3 for the former and 20% for the latter. To explain in more detail these observations, isothermal calorimetry and XRD was applied.

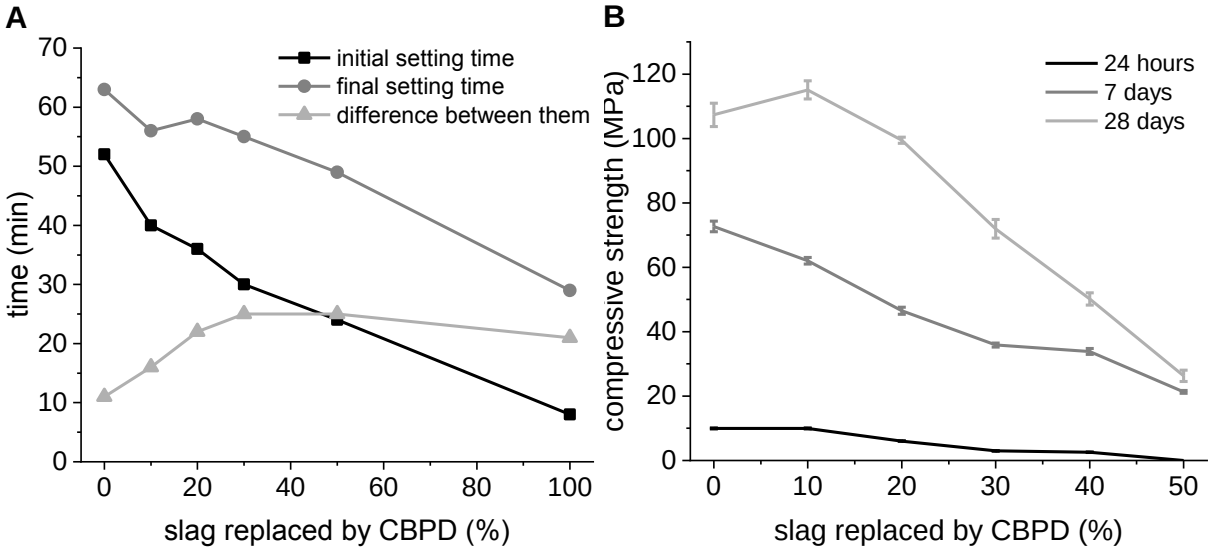

Figure 1. Effect of CBPD on setting time (A) and compressive strength (B) of AAS mixtures

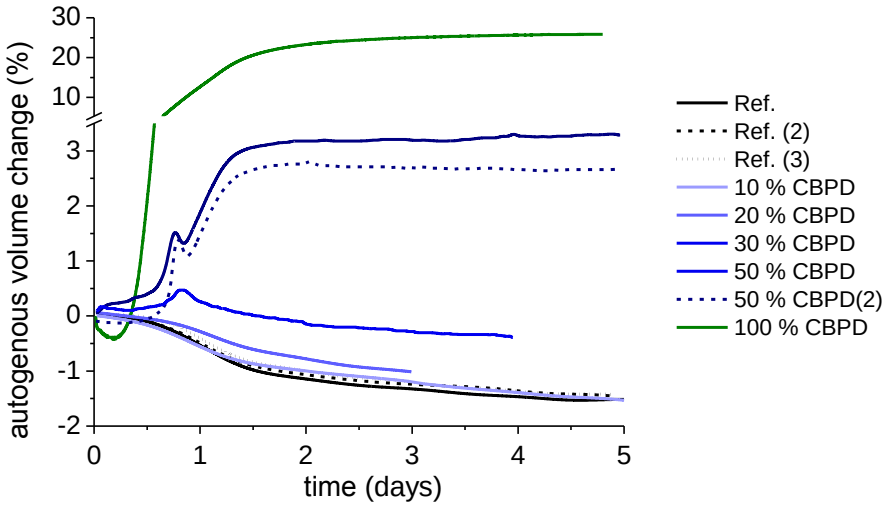

Figure 2. Effect of CBPD on autogenous volume changes of AAS pastes

Calorimetric curves of the pastes with various BFS/CBPD ratios are given in Figure 3 (heat flow) and Figure 4 (cumulative heat). It can be seen that the presence of CBPD pastes totally modified the calorimetric response of AAS paste even for the lowest used CBPD dose. The reference AAS paste showed typical calorimetric curves with three peaks described by Shi & Day (1995): The first one related to wetting and dissolution of slag particles followed by the peak of primary calcium-silicate-hydrate (C-S-H) phase formation and the last one associated with secondary C-S-H formation. However, in presence of CBPD the first peak is more intense compared to the first peak of reference

mixture, but what is even more interesting is that it is endothermic. This is due to the dissolution of phases with positive heat of solution present in CBPD, namely KCl and K_2SO_4.

Then the second peak arises, it is exothermic and its intensity increases with increasing dose of CBPD. For the paste with 25% of CBPD, this peak is followed by the third peak which correlates with the second peak of the reference mixture, while for higher CBPD doses second peak shows a shoulder but no peak simultaneous with primary C-S-H formation of the reference paste. This suggest that the second peak on curves of CBPD-containing mixtures would be related to the hydration of free lime followed by primary C-S-H formation, which thanks to high amounts of dissolved calcium ions appears earlier in pastes with high contents of CBPD and is manifested by the shoulder of the second peak.

Also the maximum of the third calorimetric peak of the reference paste appears earlier in presence of CBPD. As was already mentioned, for the reference paste this peak should be associated with secondary C-S-H formation. However, as CBPD content increases at the expense of slag and thus also the amorphous phase content decreases (although some amorphous phase would be present in CBPD), it is a question which phases are formed when this peak occurs, particularly in the pastes with high CBPD dose. One possibility is hydrocalumite, which was for BFS/CBPD pastes clearly detected using XRD after 7 days (Figure 5). Hydrocalumite belongs to wide family of AFm-type phases, whose sulfate group can be replaced by other anions like Cl^- or CO_3^{2-} (Taylor, 1990) and Al^{3+} by other trivalent kations like Cr^{3+} or Fe^{3+} (Rousselot et al. 2002).

According to Figure 5, its formation started between 24 hours and 3 days of hydration, which is somewhat later than would be expected from the onset autogenous expansion given in Figure 2, but it is also possible that its amounts were below the detection limit or its crystals were not developed enough. Also the decrease in intensity of both KCl and NaCl phases between 24 hours and 3 days support the theory about the hydrocalumite formation since they are only chloride-bearing phases in the system. Sodium and potassium are also present in the form of apthitalite, also known as glaserite, which is mineral occurring in saline deposits of lake basins and near the volcanoes (Hilmy 1953).

Some expansion can be caused also by the portlandite formation, but intensity of its peak around 18° 2θ did not change significantly throughout the testing intervals. On the other hand, free CaO content drops rapidly during the first minutes and hours (Figure 6) which would also support the theory that the second peak observed in calorimetric curves of CBPD containing pastes is associated with free CaO hydration. No significant increase in portlandite contents suggest that nascent calcium hydroxide is immediately consumed for the formation of other phases, e.g. primary C-S-H in these early stages (shoulder of the second peak on calorimetric curves of CBPD-rich pastes) or hydrocalumite and secondary C-S-H at later stages. Increasing content of C-S-H with time of hydration can be expected also from the increasing hump around the calcite peak (29,5° 2θ), where the diffractions of C-(A)-S-H phase can also be found (Myers et al. 2015, Zhang et al. 2018).

On both XRD patterns (Figure 5 and 6), many phases which were not discussed up to now can be observed. These are minerals from slag, akermanite-gehlenite and merwinite, as well as minerals from CBPD like and β-C_2S, quartz, or akermanite-gehlenite. From these phases, only β-C_2S can be hydraulically active, but its hydration is slow and moreover was also observed to be suppressed in presence of alkaline activator (Lodeiro et al. 2016). This correlates well with Figure 6, which shows that the amount of belite did not changed significantly throughout the testing period.

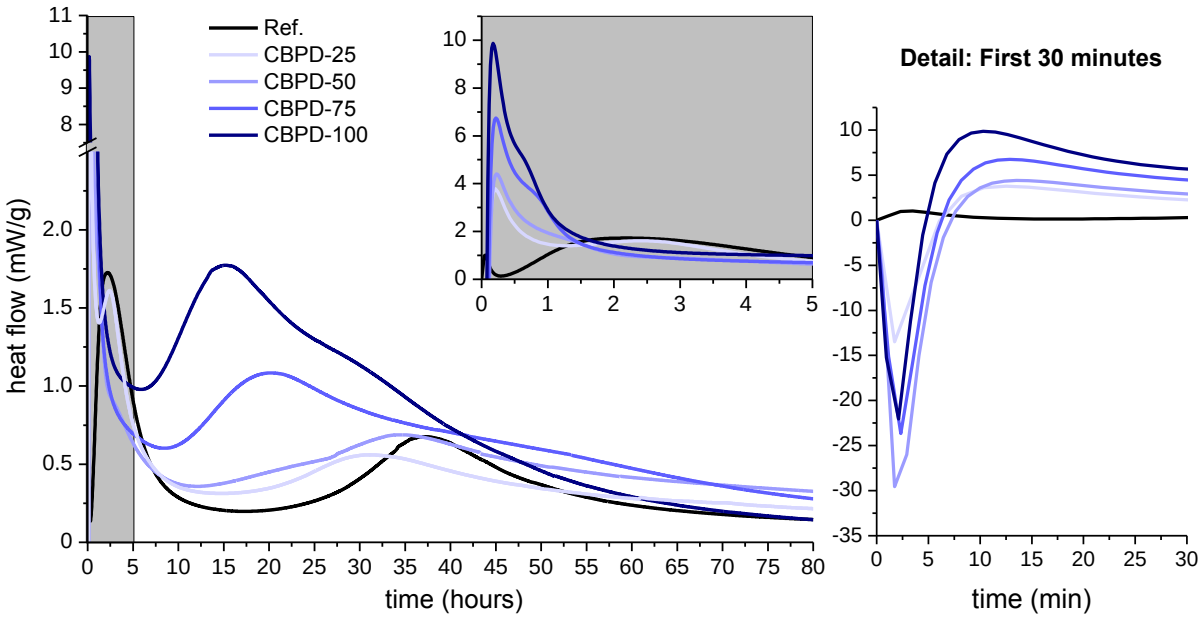

Figure 3. Effect of BFS replacement by CBPD on heat flow during the hydration of AAS pastes

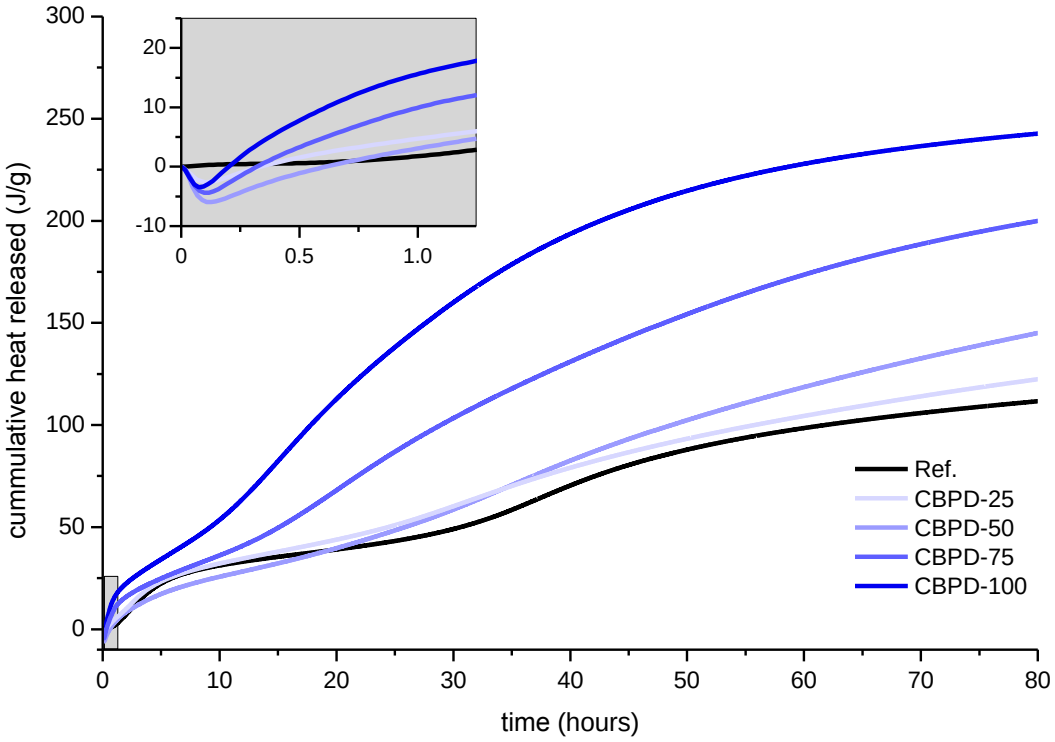

Figure 4. Effect of BFS replacement by CBPD on the heat released during the AAS pastes hydration

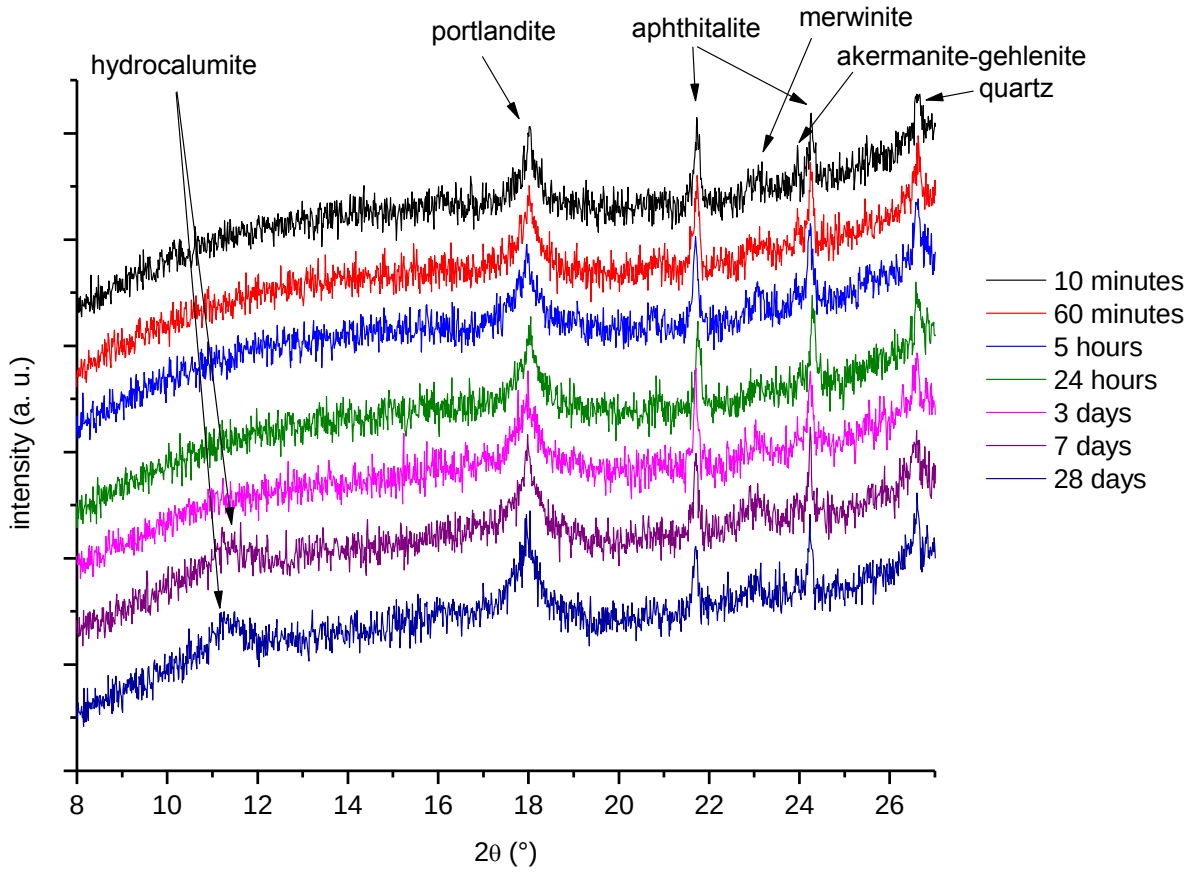

Figure 5. Part of XRD patterns (8–26° 2θ) of the paste with BFS/CBPD = 50/50

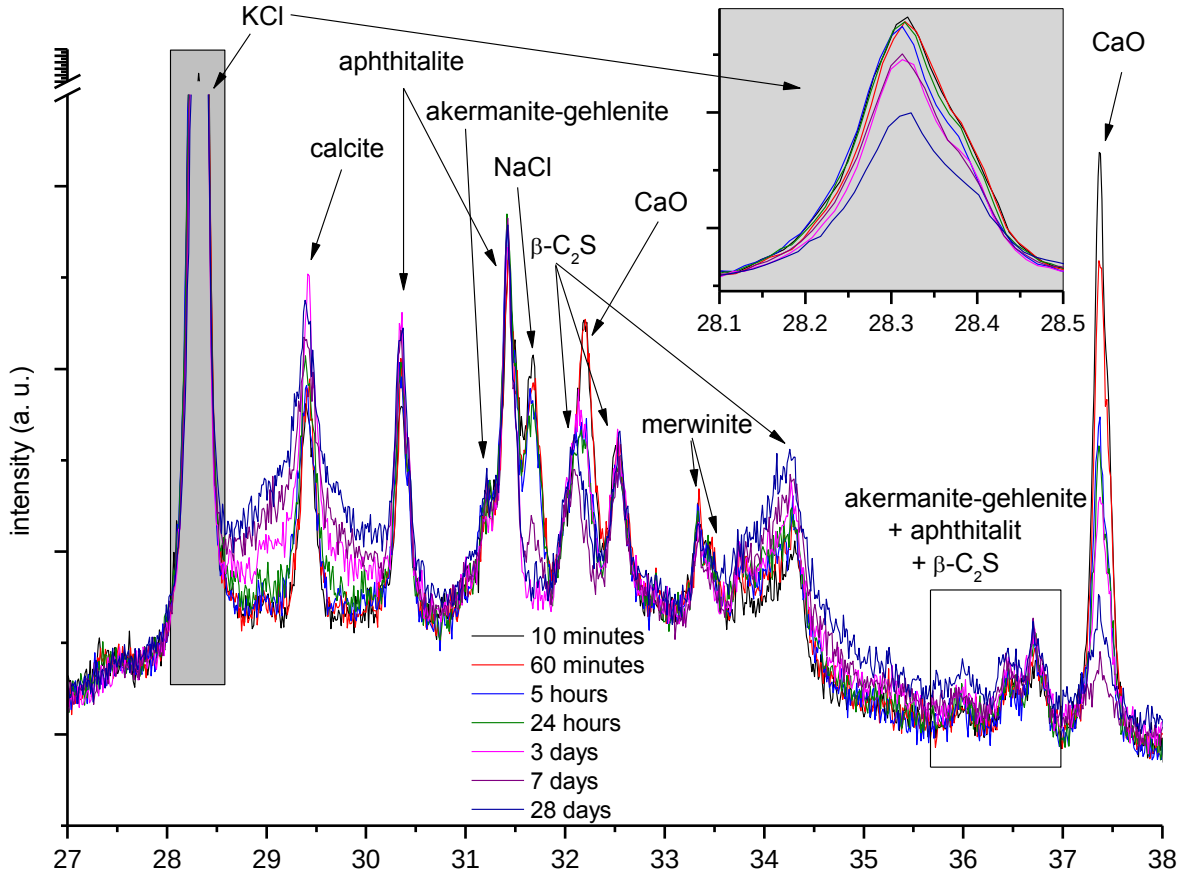

Figure 6. Part of XRD pattern (27–38° 2θ) of the paste with BFS/CBPD = 50/50

4. Conclusions

This paper investigated the effect of partial or even full BFS replacement by CBPD in waterglass-activated slag systems. It was observed that increasing dose of CBPD resulted in the decrease in compressive strength, acceleration of setting time and compensation of autogenous shrinkage of AAS mixtures up to even 25% expansion for 100% CBPD. These effects are related particularly to high free CaO and KCl contents in CBPD. They are also able to totally modify AAS calorimetric curves as well as the nature of resulting hydration products. The observed autogenous expansion seems related to formation of hydrocalumite.

5. Acknowledgements

This outcome has been achieved with financial support by the project no. 734833 “GeoDust” of H2020 call Marie Sklodowska-Curie Research Actions: Research and Innovation Staff Exchange financed by European Union funds and with financial support of the Czech Science Foundation (GAČR) under the project No 18-12289Y.

6. Appendix

Reference codes of the phases detected in alkali-activated BFS/CBPD pastes using XRD (database PDF2) are as follows:

KCl, sylvite: #01-075-0296

CaO, lime: #01-077-2376

$CaCO_3$, calcite: #01-086-0174

$Ca(OH)_2$, portlandite: #01-078-0315

$Ca_3Mg(SiO_4)_2$, merwinite: #01-089-2432

$Ca_2(Mg_{0.75}Al_{0.25})(Si_{1.75}Al_{0.25}\ O_7)$, akermanite: #01-079-2424

$Ca_2(SiO_4)$, larnite: #01-083-0461

$K_3Na(SO_4)_2$, aphthitalite: #00-020-0928

NaCl, halite: #01-070-2509

SiO_2, quartz: #01-083-0539

7. References

Aïtcin PC & Flatt RJ (2015). *Science and Technology of Concrete Admixtures*. United Kingdom: Woodhead Publishing, ISBN 9780081006931.

Garcia-Lodeiro I, Donatello S, Fernandez-Jimenez A & Palomo A (2016). *Hydration of Hybrid Alkaline Cement Containing a Very Large Proportion of Fly Ash: A Descriptive Model*. Materials 9: 605–.

Hilmy ME (1953). *Structural Crystallographic Relation between Sodium Sulfate and Potassium Sulfate, and Some Other Synthethic Sulfate Minerals*. American Mineralogist 38: 118–135.

Jin F, Gu K & Al-Tabbaa A (2014). *Strength and drying shrinkage of reactive MgO modified alkali-activated slag paste*. Construction and Building Materials 51: 395–404.

Myers RJ, L´Hopital E, Provis JL & Lothenbach B (2015). *Composition–solubility–structure relationships in calcium (alkali) aluminosilicate hydrate (C-(N,K-)A-S-H)*. Dalton Transactions 44: 13530–13544.

Rousselot I, Taviot-Gueho Ch., Leroux F, Léone P, Palvadeau P & Besse JP (2002*). Insights on the Structural Chemistry of Hydrocalumite and Hydrotalcite-like Materials: Investigation of the Series* $Ca_2M_3(OH)_6Cl{\cdot}2H_2O$ *(*M^{3+}*:* Al^{3+}*,* Ga^{3+}*,* Fe^{3+}*, and* Sc^{3+}*) by X-Ray Powder Diffraction*. Journal of Solid State Chemistry. 167: 137–144.

Shen W, Wang Y, Zhang T, Zhou M., Li J & Cui (2011). *Magnesia modification of alkali-activated slag fly ash cement*. Journal of Wuhan University of Technology-Mater. Sci. Ed. 26: 121–125.

Shi C & Day RL (1995). *A calorimetric study of early hydration of alkali-slag cements*. Cement and Concrete Research 25: 1333–1346.

Taylor HFW (1990). *Cement Chemistry*. Academic press, London. ISBN 0-12-683900-X.

Yuan X, Chen W, Lu Z & Chen H (2014). *Shrinkage compensation of alkali-activated slag concrete and microstructural analysis*. Construction and Building Materials 66: 422–428.

Zhang Z, Zhu Y, Zhu H, Zhang Y, Provis JL & Wang H (2018). *Effect of drying procedures on pore structure and phase evolution of alkali-activated cements*. Cement and Concrete Composites 96: 194–203.